JOURNAL OF MATERIALS SCIENCE 21 (1986) 2667–2677

A microscopy study of impact damage of epoxy-matrix carbon-fibre composites

D. J. BOLL, W. D. BASCOM, J. C. WEIDNER, W. J. MURRI
Hercules Aerospace, Bacchus Works, Magna, Utah 84044, USA

The damage associated with the impact of quasi-isotropic epoxy-matrix carbon-fibre composites was studied by sectioning through the impact area and photographing the polished sections. Composites with a state-of-the-art low fracture-energy matrix resin (Hercules 3501-6) and a new high fracture-energy resin (Hercules X8551) were compared. Damage in the low-toughness matrix laminate was characterized by a network of interlaminar and transverse cracking that extended some distance beyond the centre of impact. A similar network of transverse and interlaminar cracking developed in the impacted tough-matrix laminate but was largely confined to a region immediately below the impact centre. This difference in the volume of impact damage could be easily attributed to the high interlaminar fracture energy of the X8551 resin compared to the 3501-6 resin. The type and distribution of impact damage are discussed in terms of energy-dissipative mechanisms and the stress patterns that develop during impact due to mechanical deflection and stress-wave interaction. Also, the results of the sectioning study are compared with damage assessment by ultrasonic backscattering.

1. Introduction

Much of the evidence for a loss in strength of organic-matrix, carbon-fibre composites due to relatively low impact forces is the result of work by Starnes *et al.* [1] and others at the Langley Research Center (NASA). They demonstrated that the compressive and tensile strength of carbon-fibre reinforced laminates are seriously reduced by impact damage. In some instances the compressive strength was reduced by 50% or more after impact by metal projectiles at low energy levels (20 to 45 N) that produced no visible external damage. They also demonstrated that by increasing the matrix-resin fracture energy the effect of impact loading was significantly reduced.

The loss in laminate mechanical properties due to impact damage has since been confirmed by a number of workers [2–4]. Efforts to improve the "damage tolerance" of composites have been directed primarily at developing high fracture-energy resins with a minimum trade-off in other resin-controlled laminate properties. Other approaches have included variations in fibre orientation and structural design, e.g. stringers or ribs to restrict the growth of delaminations.

Various methods have been devised to determine the effect of impact on laminate strength. In the development of tough resins, where it is necessary to screen numerous formulations, relatively small panels or coupons are fabricated with specific multi directional fibre orientations, impacted over a short range of energies, and tested for residual strength This procedure has been very useful in developing damage-tolerant matrix resins and in evaluating the effect of different fibres. It is problematical as to how these data translate into the response of larger structures to impact loads.

In the work described here, small (10 cm × 15 cm × 0.5 cm) plates were impacted and then sectioned through the damage zone, and the sections examined using reflected light microscopy to determine the type and extent of damage. Two matrix resins were used, Hercules 3501-6 and Hercules X8551, where the latter has an 8 × higher fracture energy and a post-impact compressive strength 2 × greater at 109 N impact load then the 3501-6. The study revealed major differences in the extent, type and location of the damage for the two matrix materials.

2. Experimental procedure

Panels of Hercules 3501-6/IM7G and Hercules X8551*/IM7G were fabricated into 4 in. (10.2 cm) × 6 in. (15.2 cm) and 32 ply (0.5 cm) panels. The fibre orientation was $(+45/90/-45/0)_{4S}$. The pertinent properties of the resins, including cure conditions, are given in Table I. The pertinent fibre properties are given in Table II.

The plates were impacted using an ETI 630 impact drop-tower test system at an impact load of 24.6 ft-lbs (109 N). The impacter was a 0.625 in. (1.59 cm) diameter steel ball. The plate was held against an open frame as shown in Fig. 1. Note that this arrangement allows some limited flexure of the plate and also that the unsupported back-slide constitutes a low-impedance stress-wave boundary.

A set of six plates were cut from a 14 in. (35.6 cm) × 14 in. (35.6 cm) panel. All plates except one were

*X8551 was an experimental resin that has been superseded by Hercules 8551-7 resin.

0022–2461/86 $03.00 + .12

TABLE I Properties of Hercules 3501-6 and X8551 resins

Resin	Fracture energy ($J m^{-2}$)		Glass transition temperature T_g (°C)	Post-impact compression (ksi)*
	Resin	Interlaminar		
3501-6	95	180†	210	25
X8551	780	740‡	178	45

Cure Schedule: vacuum bag/autoclave, 2 h at 350° F (177° C)

*1 ksi = 6.895 MPa
†Tested in AS4 fibre.
‡Tested in AS6G fibre.

TABLE II Properties of Hercules IM7G carbon fibre

0° tensile laminate properties			Diameter (μm)
Strength (MPa)	Modulus (GPa)	Elongation (%)	
5.52	276	1.9	5.2

impacted and then tested for residual compressive strength (post-impact compressive strength, PIC, Table I). The plate that had not been compression-tested was examined by an acoustic backscatter technique [5] originally described by Bar-Cohen and Crane [6] to locate the region of greatest internal damage. A schematic diagram of the experimental arrangement is shown in Fig. 2. The transducer, which serves as both transmitter and receiver, is positioned at a small angle ($\gamma = 11°$) from the normal to the plate front surface and at a selected azimuthal angle β. Positioning the transducer at a small angle off normal incidence directs the strong front- and back-surface reflections away from the backscattered signal. The backscattered signals have a maximum amplitude when β is such that fibres or discontinuities (i.e. broken fibres, cracks etc.) are normal to the incident ultrasonic beam. Backscatter C-scans were performed at several azimuthal angles ($\beta = 0°, \pm 45°$ and 90°) on the impacted plates to produce two-dimensional maps of the damaged area.

For both the 3501-6 and the X8551 matrix materials the damage area was largely contained within a 2 in. × 2 in. area centred on the point of impact which could be readily seen on the plates. The plates were then cut and sectioned as shown in Fig. 3 It was subsequently found from the sectioning study that the damage in the 3501-6 plate extended well beyond the 2 in. × 2 in. area. The square around the damage zone was cut with a diamond cut-off saw (precision Slicing and Dicing Machine Model WMSA 1018, Micromech Mfg. Co.). A cut was then made through the centre of the damage zone using a diamond wafering saw (Buehler Isomet Low Speed Saw) with a 0.015 in. (0.38 cm) thick blade as shown in Fig. 3. One of the halves was potted in an amine (Jeffamine 230) cured diglycidylether Bisphenol A (Dow 332) epoxy with an amine accelerator (399, Texaco Chemical Co.) and a fluorescein dye (0.3 wt % Dayglo Fire Orange). The sample was covered with the liquid embedding resin, degassed at 0.25 mm Hg and then cured at ambient temperature and pressure. Excess potting resin was polished off the cut laminate surface (see below).

Slices were cut from the potted section at 0.075 in. (0.190 cm) intervals. One face of each slice was polished (Buehler Economet polisher) sequentially with Nos 320, 400 and 600 SiC grit papers followed by a 6 μm diamond paper and wet polishing with 1 μm CeO paste on a velvet cloth.

The polished surfaces were examined using reflected-light microscopy for the type and extent of damage in each ply.

3. Results

3.1. 3501-6/IM7G

The damage observed within the 3501-6 laminates was dominated by delamination between plys connected by transverse cracks through 90° and 45° plys. This network of delamination and transverse cracking is illustrated in Fig. 4. This photograph was taken from the left-hand side of a laminate slice immediately below the centre of impact. Although it shows extensive damage, the major damage in this plate occurred below the mid-plane and away from the impact centre as shown in Fig. 5. The isometric drawing in Fig. 5 presents the outer bounds of damage in each ply without any attempt to distinguish the type of damage. However, the most predominant type of damage throughout all the indicated areas was a network of interconnecting delaminations and transverse cracks (Fig. 4). To find the outer bounds of delamination it was necessary to slice and polish sections beyond the initial 2 in. square (Fig. 2).

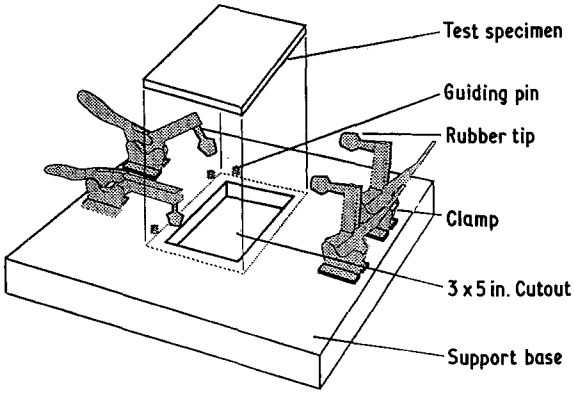

Figure 1 Impact test fixture. Size of cut out 3 in. (76 mm) × 5 in. (127 mm).

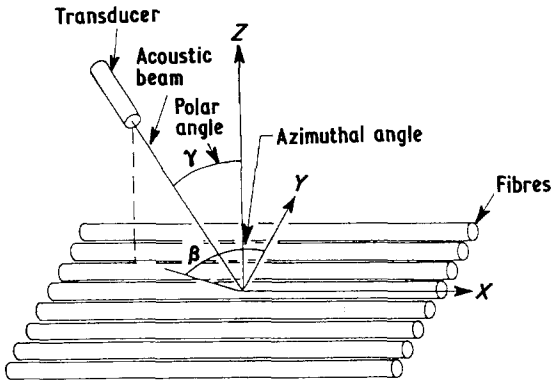

Figure 2 Diagram of experimental arrangement for acoustic backscattering from composite panels.

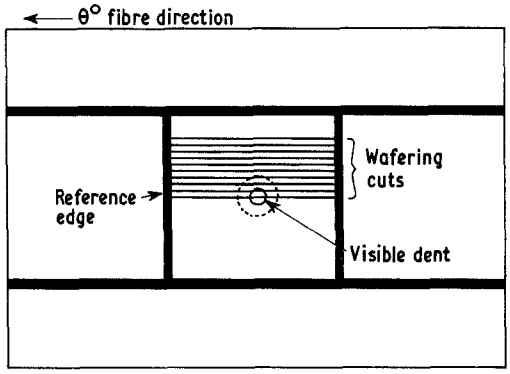

Figure 3 Sectioning diagram (impact side); location of damage was measured from reference edge (Figs 5 and 12).

The development of the interlaminar and transverse crack network appears to involve the propagation of a delamination with the coincident formation of transverse cracks which frequently, but not always, diverted the delamination through an adjacent 45° or 90° ply; but rarely through a 0° ply. In Fig. 4 it is possible to find transverse cracks that terminated without redirecting or initiating a delamination.

There was a strong tendency for the delamination to propagate in the resin-rich areas between plys but near the fibre–resin boundary as shown in Figs 6 and 7. It is reasonable that residual stresses in the resin near the fibres provided a low-energy path for propagation. Indeed, in propagating along this boundary the delamination in Fig. 7 was almost diverted into a transverse crack.

It was not always clear what caused a delamination to divert into a transverse crack. Sometimes a resin-rich pocket (as in Fig. 7) could be identified with crack redirection. From a fracture-energy point of view, the opening mode (G_I) for transverse cracking is greater than for delamination based on laminate tests [7]. However, the difference is small and could easily be reversed by local variations in fibre volume, resin heterogeneities etc. Moreover, these considerations are complicated by the effects of reflected stress waves and plate deflections as discussed below.

Although the delamination tended to propagate along fibre–resin boundaries the associated deformation did extend into the interply resin, as shown in Fig. 8. In these photomicrographs there are tear markings in the resin reminiscent of the hackle or chevron markings reported in fractography studies of carbon-fibre composite delaminations [8, 9].

3.2. X8551/IM7G

The characteristic damage of the X8551 matrix laminate included transverse cracking, delamination and fibre breakage. These features are shown in the photomicrographs in Figs 9a and b, taken from a section just below the point of impact (Fig. 9a is the left-hand side and Fig. 9b the right-hand side of the impact

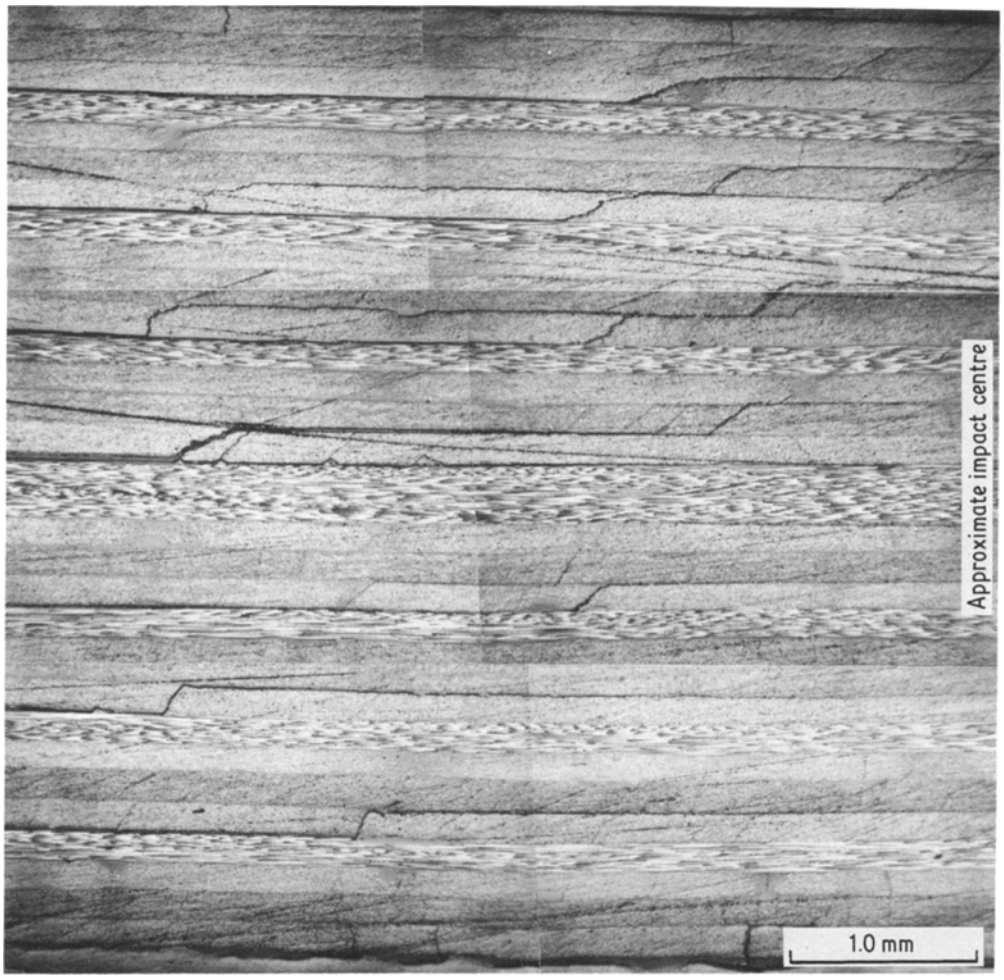

Figure 4 Impact damage in 3501-6/IM7G.

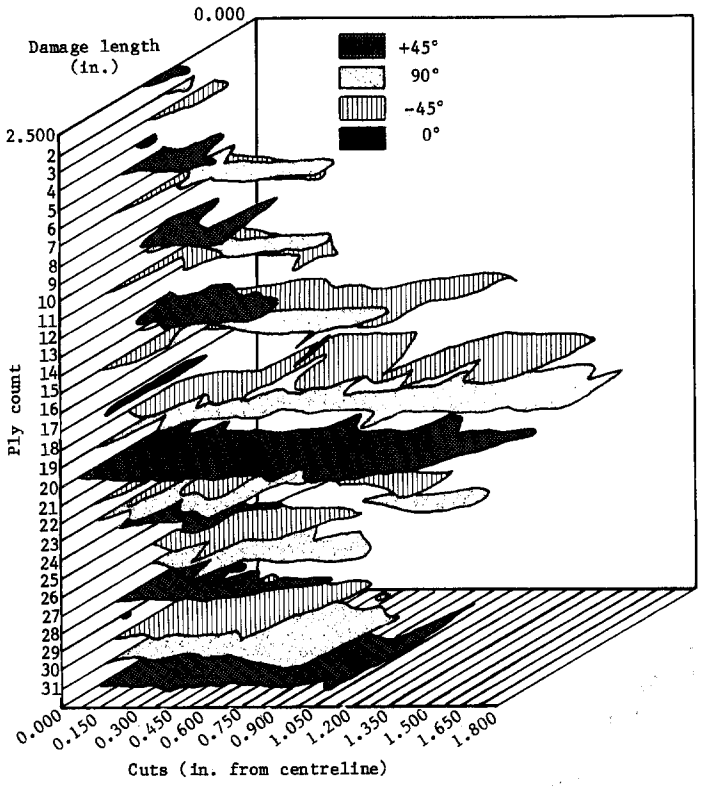

Figure 5 Damage area in 3501-/IM7G (half section). 1 in. = 25.4 mm.

centre line). The top-surface indentation had a diameter of about 0.5 in. (1.3 cm) compared to the 0.08 in. (0.2 cm) for 3501-6. Moreover, there was plastic deformation of the top ply of the X8551 matrix laminate. At the top of Figs 9a and b the 45° ply disappears near the centre of the impact zone. Visual inspection of the impact area indicated the material had been radially moved from the impact "epicentre."

The internal damage was dominated by transverse cracking with limited delamination (Fig. 10). In many instances the transverse crack propagated through adjacent plys including fibre fracture of 0° fibres (Fig. 11). Note in Fig. 11 that fibre breakage in the 0° ply included some intra-ply delamination. Also, fracture through a 0° ply often involved wide delaminations above and below the ply fracture which terminated a short distance from the break.

The most striking characteristic of the X8551/IM7G laminate was that the extent of damage was much reduced compared to the 3501-6 matrix laminate. This difference is easily seen by comparing Figs 6 and 12, and also in the plot of impact areas in Fig. 13. These plots indicate that the lateral extent of damage in the 3501-6 laminate was two or three times greater than in the X8551 material. Most of the damage in the latter near the centre of impact was transverse cracking. However, the propagation of damage away from the centre shown in Figs 12 and 13 was primarily delamination.

Occasionally, an air void was observed in a cut section. There was no evidence that damage initiated from these voids. In fact, Fig. 14 shows that the void had no influence on delamination propagation.

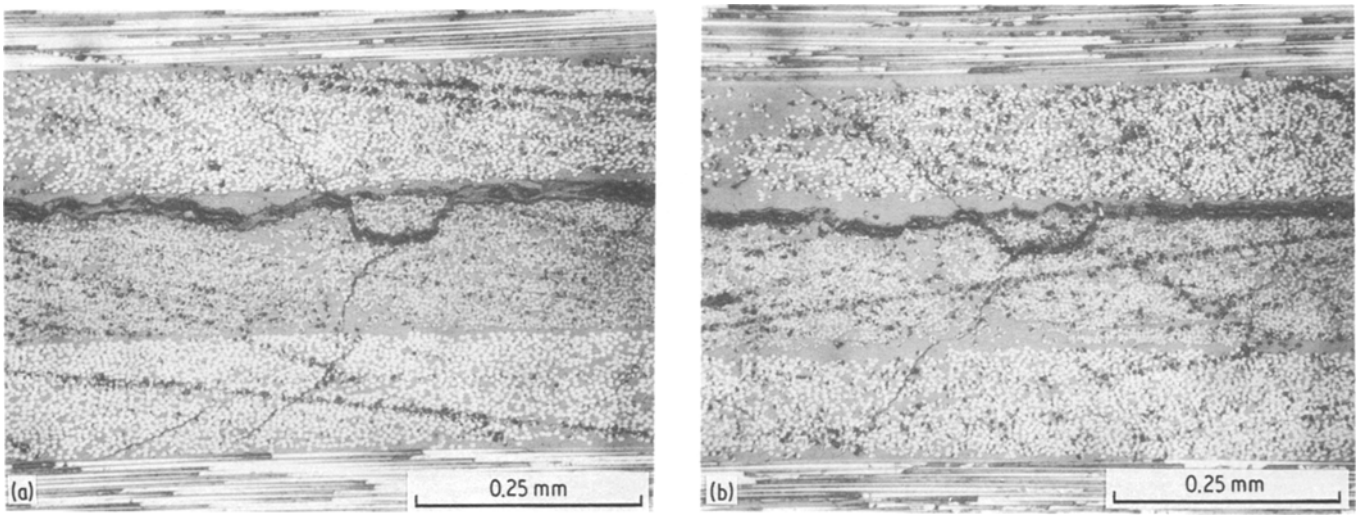

Figure 6 (a, b) Multiple-ply transverse cracking in 3501-6/IM7G.

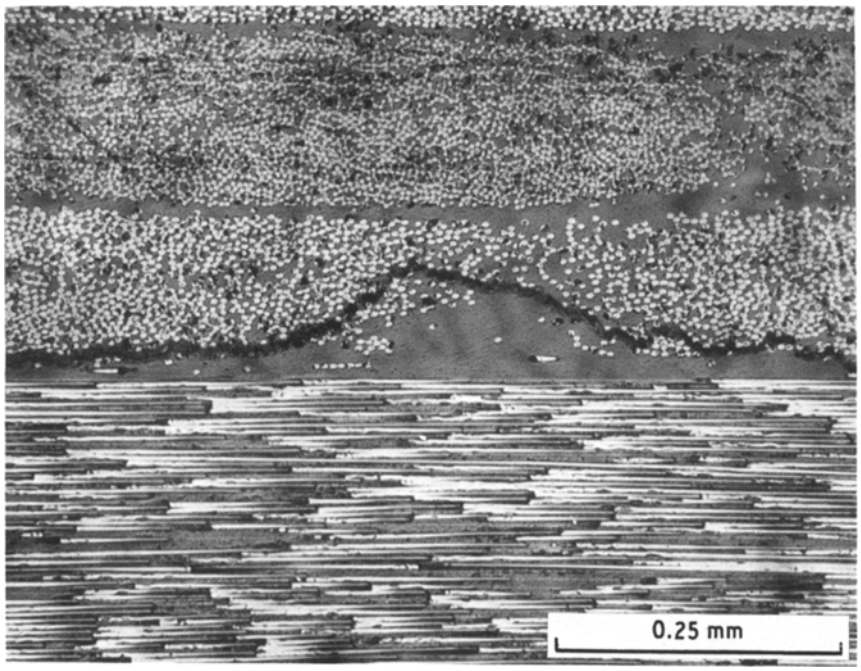

Figure 7 Propagation of a delamination at the fibre–resin boundary in 3501-6/IM7G

3.3. Ultrasonic backscattering

Microsectioning, polishing and microscopy is a destructive and very laborious method of determining impact damage. However, there are no non-destructive methods of characterizing this damage in as much detail as can be obtained by sectioning. An acoustic backscattering technique [5, 6] is capable of determining variations in the extent of damage within a laminate, both in depth and radially from the impact centre. This technique for producing backscatter C-scans is being developed [5] and was used here to supplement the sectioning study and to indicate directions to improve the acoustic technique to better characterize internal damage.

The C-scan results are presented in two formats in Figs 15 and 16 for the 3501-6 matrix laminate and the X8551 laminate, respectively. The shaded dot-patterns indicate the damage within the 2 in. (5.1 cm) square area denoted in Fig. 2. The shading intensity is proportional to the amount of *total* damage through the laminate thickness. The shaded maps were replotted as three-dimensional maps of backscatter energy as shown in Figs 15 and 16. The cut made through the 2 in. square is indicated on the three-dimensional plots and sections were sliced from the back portion of the cut.

The C-scan plots indicate a number of features also revealed by microsectioning. The much larger diameter of the damaged area in the 3501-6 matrix laminate compared to the X8551 matrix laminate is evident in comparing Figs 15 and 16. The damage was most severe directly under the point of impact for the X8551 resin. The damage was most widely spread for the 3501-6 resin laminate. The maximum damage on the 3501-6 matrix plate is slightly off-centre in Fig. 15, suggesting that the impact load was not precisely normal to the plane of the laminate. Microsectioning confirmed that the damage through the laminate was not symmetrically distributed. Fig. 15 indicates that all the damage in the 3501-6 matrix laminate did not

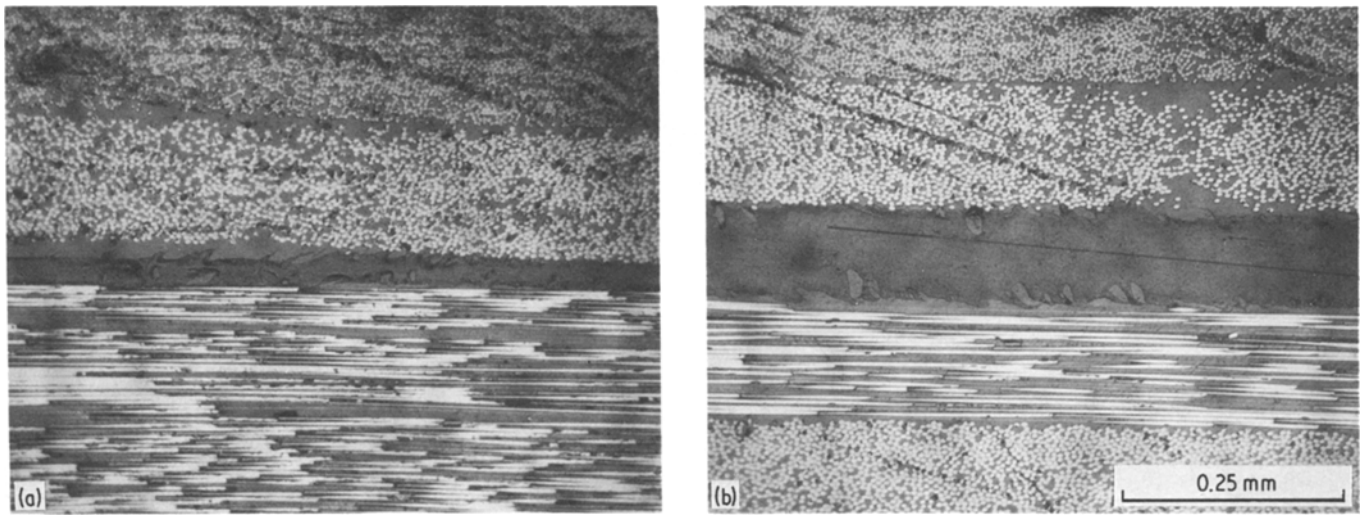

Figure 8 (a, b) Resin tearing associated with delamination of 3501-6/IM7G.

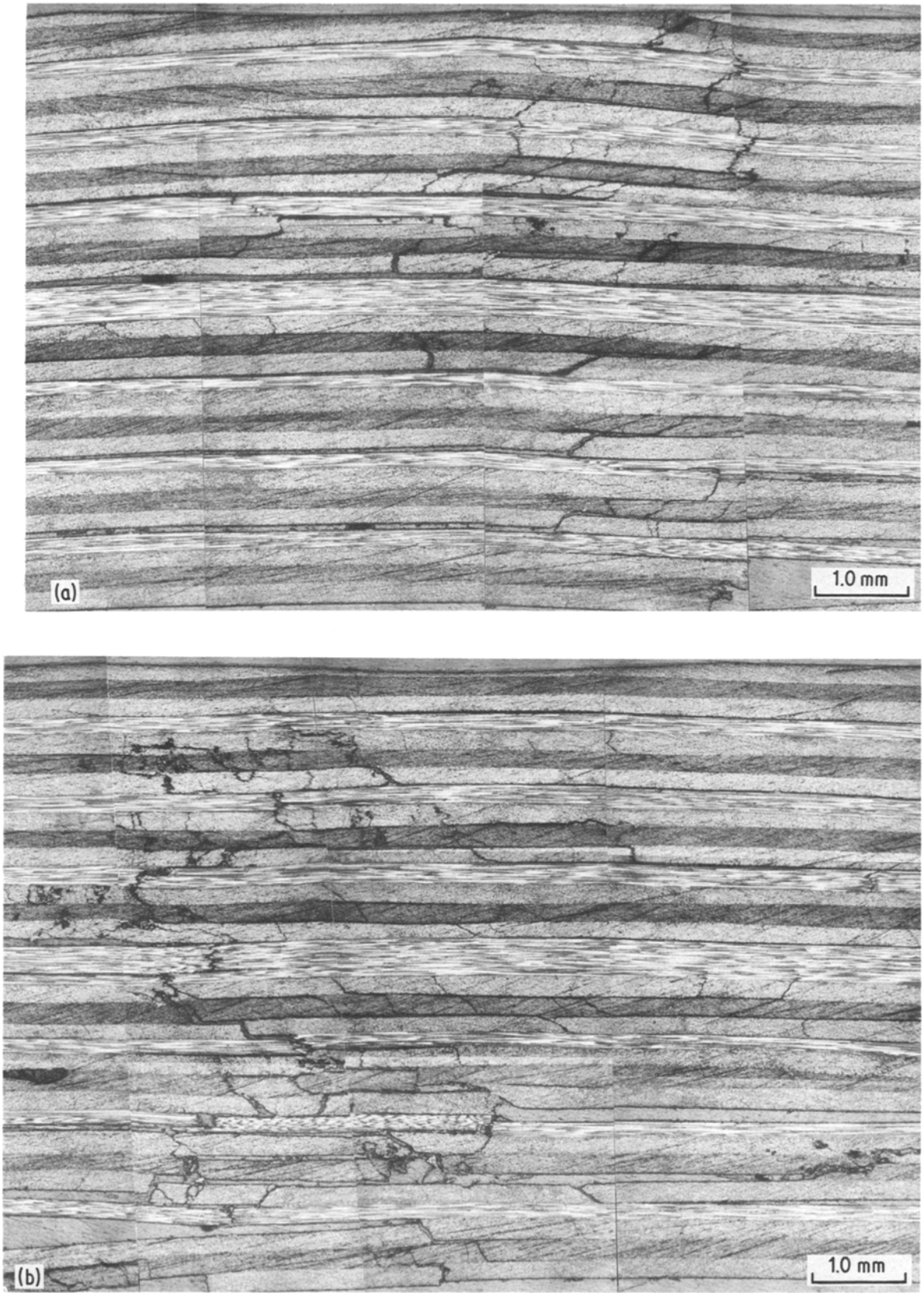

Figure 9 Damage in 8551/IM7G: (a) left-hand, (b) right-hand side.

radiate from the impact centre. Areas of damage, some of which extended beyond the 2 in. square area, developed without any apparent initiation from the region of maximum damage. Similar isolated damage areas can be found on the map (Fig. 5) developed from the sectioning study. In some instances these isolated damage areas resulted from delamination being redirected by transverse cracking which went undetected by the C-scan. None the less, compared to a conventional (normal-incidence) C-scan the backscatter technique used here is more sensitive and yields significantly more information about damage distribution.

The principle deficiency of the backscatter C-scan

Figure 10 Transverse cracking in 8551/IM7G.

technique in its present state of development is that the signal gives a summation of damage through the laminate thickness. Work is in progress here to process this signal for changes in intensity as a function of penetration depth.

4. Discussion

Impact damage in the 3501-6 matrix laminate was dominated by delamination and transverse cracking that extended well beyond the centre of impact, out to ~4 cm (1.7 in.). In sharp contrast, the X8551 damage was dominated by transverse cracking, local delamination and fibre breakage within 1.8 cm (0.7 in.) of the impact centre. These differences are attributed to the higher fracture energy of the X8551 resin compared to the 3501-6 resin (Table I).

The damage in the 3501-6 laminate was characterized by a network of interconnecting delaminations and transverse cracks. It appears that this network forms by the growth of delaminations away from the impact centre that are redirected into transverse cracks, due to local conditions that cause transverse propagation to be energetically favoured. Rarely did a transverse crack continue into the next ply. To do so would require a reorientation of the crack front, e.g. from a path parallel to the 45° fibres to a path parallel to 90° fibres, which would require more energy than to initiate a new delamination. In some cases the delamination branched into a transverse direction rather than being totally diverted. This branching may occur when the delamination growth rate exceeds the material's capacity to dissipate strain energy, i.e. the Yoffe effect [10].

Interlaminar cracking was further favoured by an apparent low-energy path along the boundary between the fibres and the resin. Presumably, residual thermal stresses near the fibres reduce the local fracture energy below that of the resin itself.

In the higher fracture-energy X8551 laminate the bulk of the damage was concentrated near the impact centre. This damage, like that in 3501-6, was predominately a network of interconnecting delaminations and transverse cracks. However, the high resin toughness prevented the propagation of the delaminations away from the impact centre. Instead, the impact energy was consumed by cross-ply transverse cracking which, as already mentioned, requires a reorientation or twisting of the crack front. This reorientation of the crack is a high-energy process and reflects the high level of strain energy available which, because of the resin toughness, cannot be dissipated by delamination.

The high energy density near the centre of impact also caused fibre breakage and cracking through the 0° plys in the X8551 matrix laminate. It is not obvious why fibre fracture, which generally involves fracture energies two to three times greater than interlaminar fracture [11, 12] should be favoured over delamination. Fibre breakage was usually accompanied by local interply separation (Fig. 11), which suggests some competition between fibre fracture and interlaminar fracture.

These rationalizations of impact damage in terms of

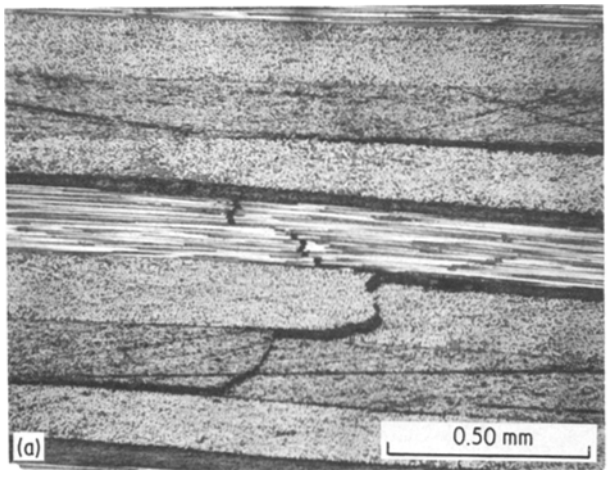

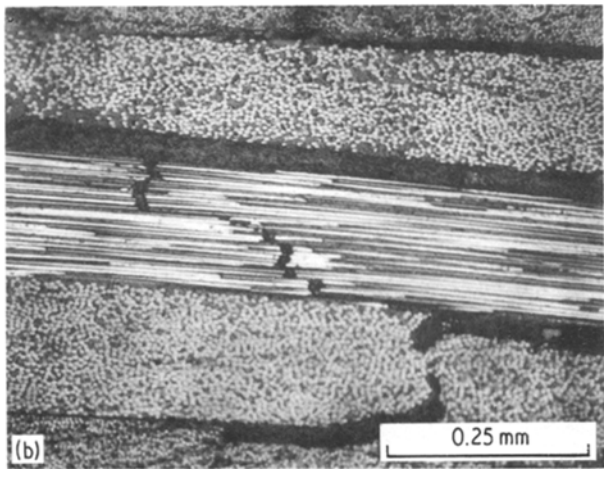

Figure 11 (a, b) Transverse cracking in 0° plys of 8551/IM7G.

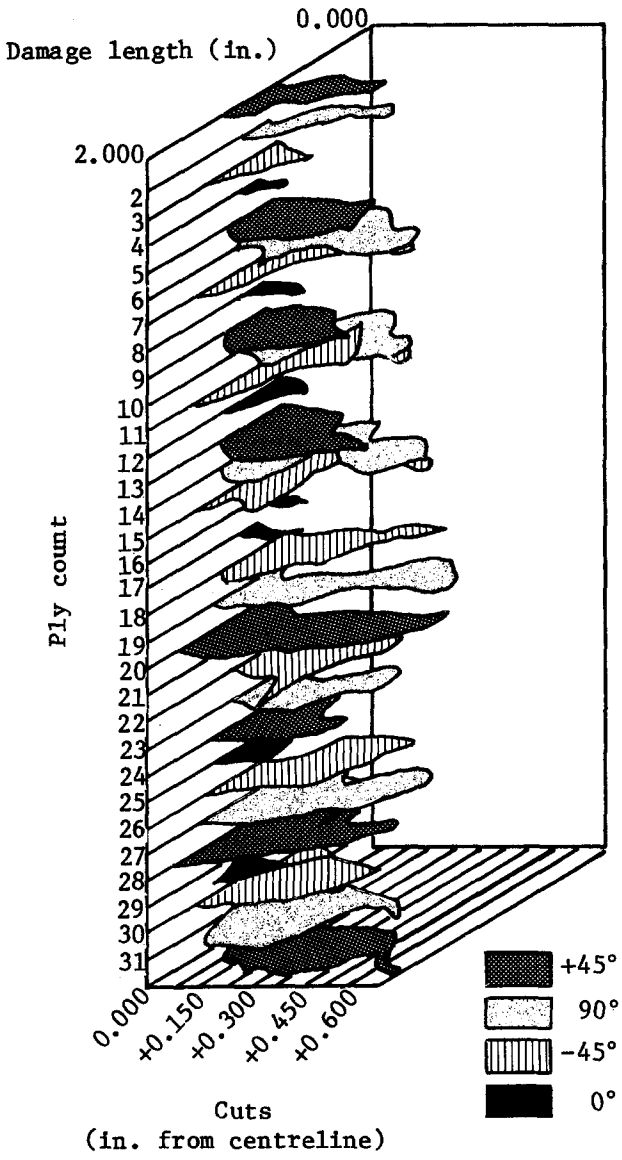

Figure 12 Damage area in 8551/IM7G. 1 in. = 25.4 m.

quasi-static fracture energies (primarily $\mathcal{G}_{Ic}$) are compelling in their simplicity but must be tempered by the actual complexity of the impact dynamics. One obvious reservation is that by sectioning in only one plane – parallel to the plys designated as 0° in the lay-up sequence – we are presuming that damage is symmetrical about the point of impact and that a similar damage pattern would be observed at any other sectioning angle. Where damage is primarily delamination and transverse cracking, the mapping of damage occurs along paths of least resistance by the high strain-energy density available for crack damage. However, narrow delaminations within 0° plys would be difficult to detect. Also, transverse cracks parallel to the cutting direction would be missed. The latter could be important in the case of the X8551 matrix laminate.

The dynamic stresses that develop during impact are complex, especially in an organic matrix composite. Greszczuk [13, 14] has reviewed this subject and analysed the compressive stress (Z, θ, r) and shear stresses ($\tau_{r,Z}$) as defined in Fig. 17. We would not expect the compressive stresses to induce the type of damage observed here (except as reflected normal stresses discussed later). On the other hand, shear stress, as shown in Fig. 17 taken from Greszczuk [13], could easily induce transverse cracking. Note in Fig. 17 that the maximum shear stresses are displaced below and away from the impact centre; at about $r/a = 1.0$ and $Z/a = 0.4$ where a is the radius of the area of contact. Inspection of Fig. 4 and Figs 9a and b suggests a concentration of transverse damage below the top surface and radially displaced from the impact centre. These concentrations of damage are not displaced as far from the impact centre as predicted by the analysis. None the less, it is reasonable to assume that crack initiation begins in this high

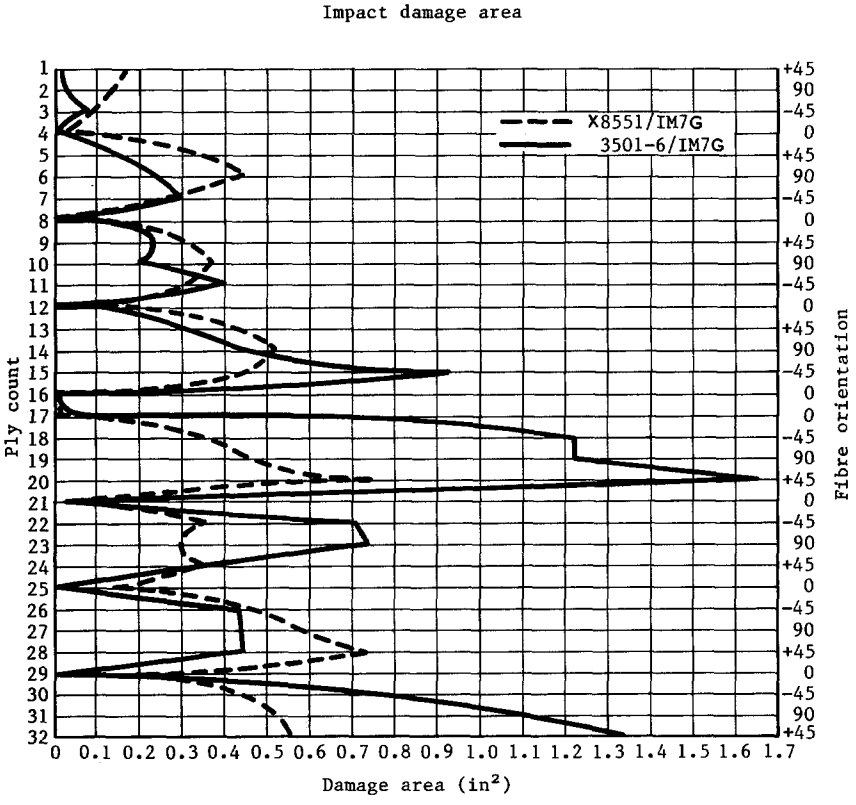

Figure 13 Impact damage areas: (– – –) 8551/IM7G, (——) 3501-6/IM7G. 1 in². = 645 mm².

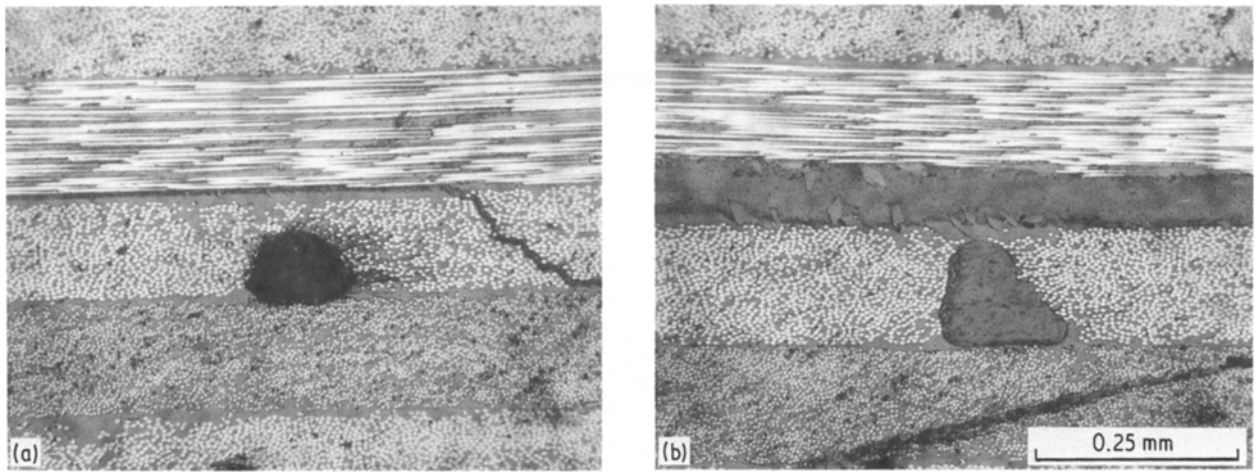

Figure 14 (a, b) Influence of voids on impact damage in 3501-6/IM7G.

shear-stress region as transverse cracks. Subsequent damage occurs along paths of least resistance by the high strain-energy density available for crack propagation.

Other important features of the impact dynamics are the reflected tensile stress wave and the bending displacement of the laminate which would produce tensile stresses (σ_z) below the laminate mid-plane. These tensile stresses may initiate delaminations, especially in the 3501-6 matrix. In Figs 5 and 12 the maximum extent of damage, primarily delamination, is below the mid-plane (ply 16). Moreover, a simple calculation of stress-wave reflections indicates a maximum tensile stress development beginning at about ply 25. This estimate is consistent with the plots of impact damage area for both 3501-6 and X8551 matrix laminates (Figs 5, 12 and 13).

In the absence of pre-existing flaws, it seems doubtful that tensile stress waves or bending stresses are large enough to initiate cracking. More likely, these stresses reinforce the propagation of delamination or transverse cracks already formed by shear stresses. Two possible examples are crack branching in the 3501-6 laminate and multiple-ply transverse cracking in the X8551 laminate.

It is clearly evident why the post-impact compressive strength of the 3501-6 laminate is significantly lower than that of the X8551 system. Due to the extensive delamination the plys are loaded independently and the laminate literally fails like a deck of cards. A similar failure mode may occur in the X8551 laminate, but the stresses for ply buckling and delamination growth) would be much higher. One aspect of post-impact compressive failure brought out by this study is that in toughening the matrix to reduce delamination there is a concentration of strain energy under the impact area which causes fibre fracture in the 0° plys. Fibre fracture in the 0° plys as well as multiple-ply transverse cracking will seriously reduce the laminate resistance to compressive loads.

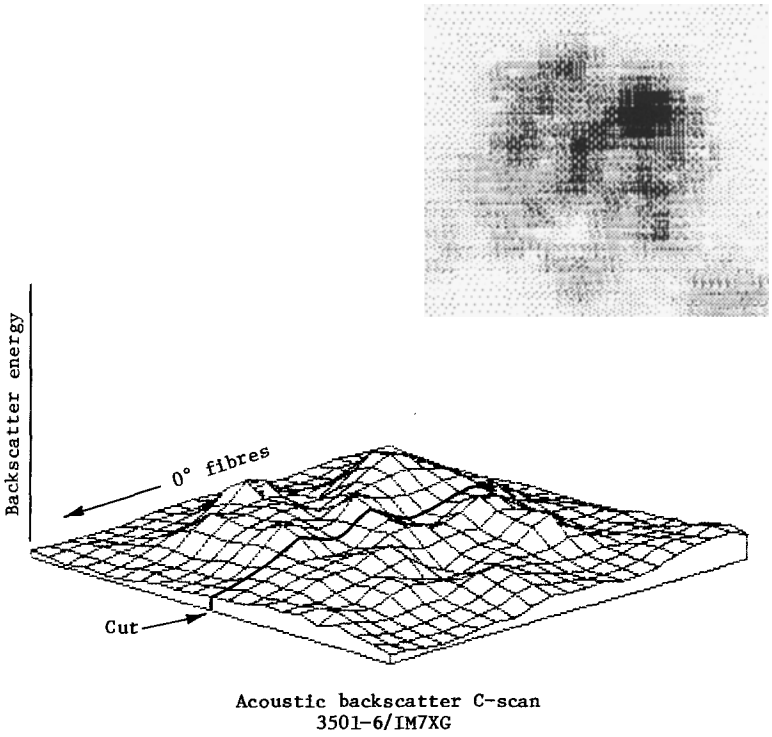

Figure 15 Acoustic backscatter C-scan for 3501-6/IM7G. Target area is 2 in. (5.1 cm) square.

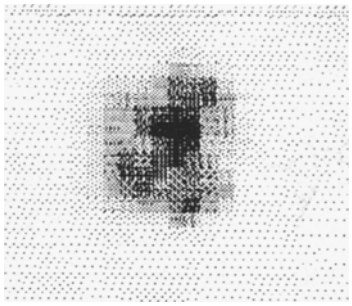

Figure 16 Acoustic backscattering C-scan for X8551/IM7G. Target area is 2 in. (5.1 cm) square.

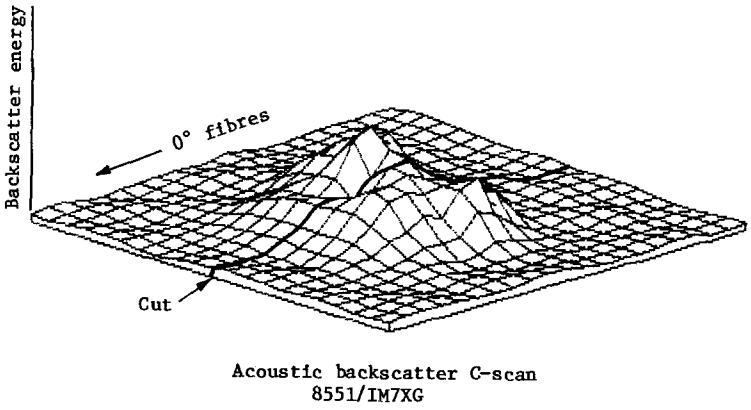

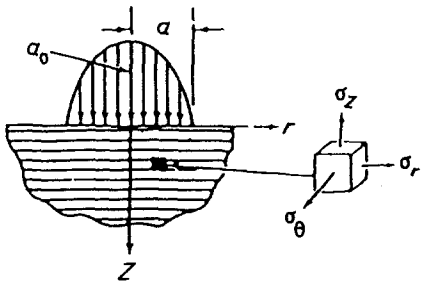

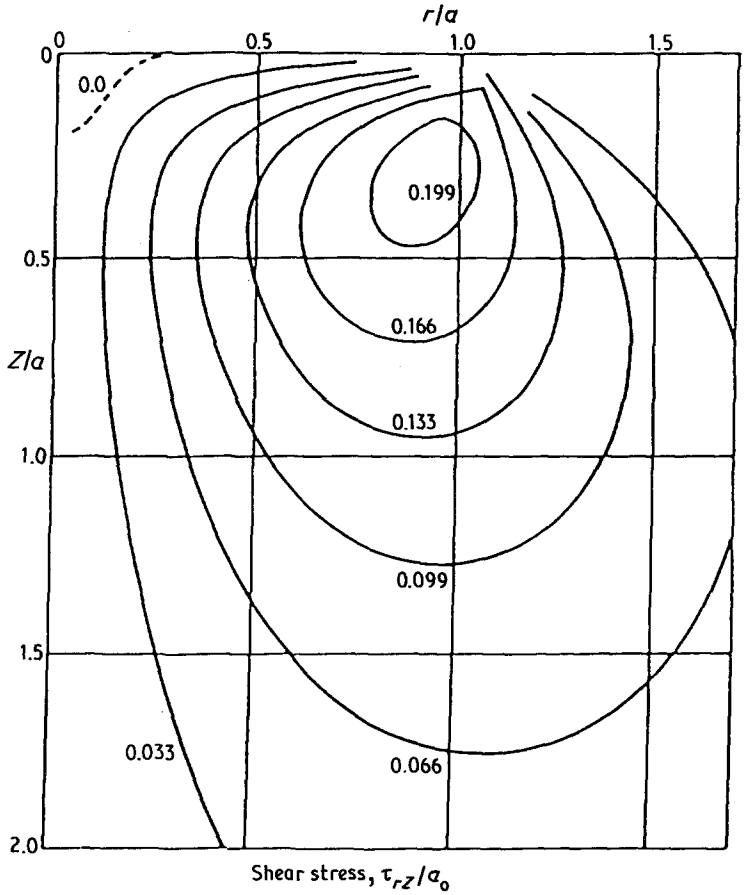

Figure 17 Stress coordinates and shear-stress distribution at impact of a metal sphere on a pseudo-isotropic glass-epoxy laminate [13].

This comparison of the different types of impact damage in high fracture-energy as against low fracture-energy matrix composites suggests two important conclusions. First, that the fibre strength becomes increasingly important as the matrix-resin toughness is increased. Second, that there may be a limit to which PIC strength can be increased by increasing the toughness of the matrix resin (for a given impact energy). When the matrix has a sufficiently high fracture energy to prevent delamination, then the post-impact strength is determined by transverse cracking and fibre fracture. There is some evidence [2] for a limit in matrix $\mathcal{G}_{Ic}$ above which the increase in post-impact compressive strength is minimal. The issue is complicated by the fact that resin shear strength and mode I fracture energy are not independent. It is quite possible that increasing $\mathcal{G}_I$ beyond the level necessary to essentially eliminate delamination would also increase resin shear strength and improve the laminate resistance to transverse cracking.

5. Conclusions

The results of this study comparing impact damage in a low fracture-energy matrix carbon-fibre composite with the damage in a high fracture-energy matrix composite indicate that:

1. The area of damage through the entire thickness of the laminate was much greater (4 to 5 ×) for the low fracture-energy matrix resin.
2. The internal damage in the low fracture-energy composite was characterized by an extensive network of delaminations and transverse cracks.
3. The internal damage in the high fracture-energy composite was characterized by multiple-ply transverse cracks, fibre breakage and localized delaminations.
4. Most of the damage characteristics can be explained in terms of quasi-static fracture mechanics.
5. Crack initiation appears to result from shear stresses developed during the early stages of impact.
6. The principle effect of normal stress-wave reflection and laminate bending is the propagation of cracks already formed by shear failure.
7. As the fracture energy of the matrix resin is increased, the fibre strength will play an increasing role in impact damage and post-impact residual strength.
8. There may be an upper limit in matrix fracture energy beyond which the post-impact compression strength is only marginally improved (for a given impact loading).
9. As the upper limit in matrix fracture energy is increased, the shear strength of the resin may become the controlling factor in impact damage.

Acknowledgements

This work was fully supported by Hercules Inc., IR&D funding. We wish to thank Dr L. H. Pearson for very helpful discussions during the course of this work.

References

1. J. H. STARNES, M. D. RHODES and J. G. WILLIAMS, ASTM STP 696 (American Society for Testing and Materials, Philadelphia, 1979) p. 145.
2. T. F. JONAS and R. F. SIEGMUND, in Proceedings of 5th SAMPE Technology Conference, Montreux, 1985 (Society Advancement of Material and Process Engineering). Paper 5.
3. W. J. CANTWELL and J. MORTON, *Compos. Struct.* **3** (1985) 241.
4. S. M. BISHOP, *ibid.* **3** (1985) 295.
5. W. J. MURRI, B. W. SERMON and L. H. PEARSON, in Proceedings of 15th Symposium on Nondestructive Evaluation, San Antonio, April 1985 (American Society of Non-Destructive Testing/Southurst Research Institute).
6. Y. BAR-COHEN and R. L. CRANE, *Mater. Eval.* **40** (1982) 970.
7. W. L. BRADLEY and R. N. COHEN, in Proceedings of ASTM Symposium on Delamination and Debonding of Materials, Pittsburg, 1983.
8. W. D. BASCOM, D. J. BOLL, B. FULLER and P. J. PHILLIPS, *J. Mater. Sci.* **20** (1985) 3184.
9. J. M. SINCLAIR and C. C. CHAMIS, "Mechanical Behavior and Fracture Characteristics of Off-Axis Fiber Composites I, Experimental Investigation," NASA Technical Paper 1081 (NASA, Washington, DC, 1977).
10. E. H. YOFFE, *Phil. Mag.* **42** (1951) 739.
11. H. J. KONISH, J. L. SWEDLOW and T. A. CRUSE, *J. Compos. Mater.* **6** (1972) 114.
12. W. D. BASCOM, J. L. BITNER, R. J. MOULTON and A. R. SIEBERT, *Composites* (January 1980) 9.
13. L. B. GRESZCZUK, ASTM STP 568 (American Society for Testing and Materials, Philadelphia, 1975) p. 183.
14. *Idem,* in "Impact Dynamics", edited by J. A. Zukas, T. Nicholas, H. F. Swift, L. B. Greszcuzuk and D. R. Currin (Wiley, New York, 1982) p. 55.

Received 13 August
and accepted 18 September 1985